JOURNAL OF Applied Polymer SCIENCE

Compatibilization of Bentonite Filled Ethylene-Propylene-Diene Monomer Composites: Effect of Maleic Anhydride Grafted EPDM

H. Ismail, M. Mathialagan
Division of Polymer Engineering, School of Materials and Mineral Resources Engineering, Engineering Campus, Universiti Sains Malaysia, Nibong Tebal 14300, Penang, Malaysia
Correspondence to: H. Ismail (E-mail: hanafi@eng.usm.my)

ABSTRACT: Maleic anhydride grafted ethylene-propylene-diene monomer (MAH-*g*-EPDM) was prepared by peroxide-initiated melt grafting of MAH onto EPDM using a HAAKE internal mixer at 180°C and 60 rpm for 5 min and it was used as compatibilizer to enhance the compatibility of EPDM/Bt composites. The composites were prepared using a laboratory scale two roll mill, model XK-160 at room temperature. The addition of 10 parts per hundred rubber (phr) of MAH-*g*-EPDM into EPDM/Bt composite results in significantly improved tensile properties compared with the uncompatibilized EPDM/Bt composites. Curing behavior, tensile properties, solvent resistance, and the rubber-filler interaction of compatibilized and uncompatibilized EPDM/Bt composites were investigated. The cure time (t_{90}), scorch time (t_{S2}), maximum torque (M_H), and minimum torque (M_L) of compatibilized composites were increased upon addition of MAH-*g*-EPDM. Compared with uncompatibilized EPDM/Bt composites, the tensile properties, solvent resistance, and rubber-filler interaction of compatibilized EPDM/Bt composites were all improved. SEM micrographs of tensile fractured surfaces of compatibilized EPDM/Bt composites showed a better dispersion of Bt and interfacial adhesion between EPDM and Bt compared with uncompatibilized EPDM/Bt composites. © 2012 Wiley Periodicals, Inc. J. Appl. Polym. Sci. 000: 000–000, 2012

KEYWORDS: bentonite; EPDM; curing behavior; tensile properties; solvent resistance

Received 27 April 2011; accepted 24 February 2012; published online
DOI: 10.1002/app.37606

INTRODUCTION

Ethylene-propylene-diene monomer (EPDM) has attracted much attention and shows a tremendous market growth among the synthetic rubber for both general purpose and specialty applications. EPDM possesses excellent resistance to heat, aging, and oxidation due to its saturated backbone. The nonpolar nature of EPDM attributes to the high electrical resistivity and excellent resistance to polar solvents and several chemicals such as brake fluid and glycol.[1] Besides that, EPDM has high mechanical and dynamic properties as well as low temperature flexibility and the ability to accept high loading of fillers, reinforcing materials, and plasticizers. Such cumulative property makes EPDM the most suitable rubber for outdoor applications, building profiles, automotive application, electrical power cable insulations, roofing sheets, and sporting good.[2–9] Reinforcing materials such as carbon black, silica, and clay minerals are commonly used as filler to improve the mechanical and thermal properties as well as to reduce cost and sometimes the weight of the rubber compounds.[10–15] Clay minerals were admirably suited as filler materials in rubber compounding due to their abundance, availability, low cost, and a good surface properties.[16]

For decades, various researches on EPDM/clay have been carried out and were found to be valuable. EPDM/clay hybrid with montmorillonite prepared by Usuki et al.[17] shows improvement on tensile strength and storage modulus and the permeability decreased 30% compared with the unfilled EPDM. Other studies by Vu et al.,[18] Kresge and Lohse,[19] and Chang et al.,[20] revealed a great improvement in properties by incorporation of clay into epoxidized natural rubber (ENR), 1,4-polyisoprene (synthetic) natural rubber, and EPDM, respectively. However, it was found that incorporation of certain mineral clays especially montmorillonite changes the character of EPDM due to the difference in polarity of the individual system and high interaction between EPDM and clay is hardly achieved unless a suitable compatibilizer is used.[21]

In a previous study,[22] bentonite (Bt) which is a type of montmorillonite was introduced into EPDM rubber as filler and the effect of Bt loading on the curing behavior, tensile, and thermal properties as well as the morphological characteristics were

studied. Result obtained for tensile and thermal properties showed an improvement with increasing Bt loading of EPDM/Bt composite compared to the pristine EPDM. However, due to saturated backbone and nonpolar nature of EPDM, it was found that Bt does not show the best interaction and was incompatible to EPDM.

Grigoryeva and Kocsis[23] have reported the melt grafting of maleic anhydride (MAH) onto EPDM which can be used successfully as compatibilizer[24,25] or in dispersed phase[26] of polymer blend to improve the properties of the blends. Manjhi and Sarkhel[1] reported the enhancement of filler–matrix bonding and the filler distribution of EPDM/kaolin with the incorporation of maleic anhydride grafted ethylene-propylene-diene monomer (MAH-*g*-EPDM) as compatibilizer. Meanwhile, Pasbakhsh et al.[27] reported similar finding at which incorporation of MAH-*g*-EPDM act as compatibilizer by creating an interphase between the EPDM and halloysite nanotubes which produces a stronger interfacial interaction and also improves the dispersion of halloysite nanotubes in EPDM matrix.

The first aim of this study is to prepare MAH-*g*-EPDM via peroxide-initiated melt grafting of MAH onto EPDM as reported by Grigoryeva and Kocsis[23] and to use it as compatibilizer in EPDM/Bt composites. Further aim would be to investigate the effect of MAH-*g*-EPDM compatibilization on the curing behavior, tensile properties, morphological characteristic, solvent resistance, and rubber-filler interactions of EPDM/Bt composites in comparison with uncompatibilized EPDM/Bt composites at various Bt loading, i.e., 5, 10, 30, 50, and 70 parts per hundred of rubber (phr).

EXPERIMENTAL

Materials

EPDM, 778Z with ethylene content of 67%, ENB of 4.3%, and ML (1 + 4) 125°C of 63 MM was purchased from Keltan DSM Elastomers. The density of EPDM, measured by a Precisa (XT220A), was 0.823 g cm^{-3}. Bentonite (Bt) was supplied by Ipoh Ceramics (M) Sdn. Bhd. The elemental composition of bentonite obtained with Rigaku RIX3000 X-Ray Fluoroscence Spectrometer (XRF Spectrometer) is listed in Table I. The physical properties of Bt were analyzed using a Malvern Mastersizer and the average particle size and specific surface area of Bt were 0.82 μm and 2.6766 sq m/g, respectively. After 24 h drying at 80°C in vacuum oven, the density of Bt was found to be 2.513 g cm^{-3}, measured by a Micromeritices, Accupyc 1330 (gas pycnometer). MAH, dicumyl peroxide (DCP) and other compounding ingredients such as zinc oxide, stearic acid, tetramethyl thiuram disulphide (TMTD), 2-mercapto benzothiazole (MBT), and sulfur were all obtained from Bayer (M) Sdn Bhd, Penang, Malaysia.

Melt Grafting of EPDM

The melt grafting of MAH onto EPDM was done in the presence of peroxide initiator using a HAAKE internal mixer at 180°C and 60 rpm for 5 min which were based on Grigoryeva and Karger-Kocsis[23] and Pasbakhsh et al.[27] who have reported them as the optimum conditions to obtain the maximum grafting of MAH onto EPDM. Materials compositions for MAH-*g*-EPDM preparation are as follows: 39 g of EPDM, 2.5 wt % of MAH and 0.25 wt % of DCP. The mixing is done in a HAAKE internal mixer with an optimum mixing volume of 44.1 cm^3 at which all the reactants (EPDM, MAH, and DCP) were dry mixed together before fast (<1 min) introduction into the preheated mixing chamber.

Table I. Elemental Compositions of Bentonite

Bentonite content	Amount (%) (w/w)
SiO_2	76.0
Al_2O_3	15.0
MgO	2.7
CaO	2.0
Fe_2O_3	2.0
K_2O	1.2
Na_2O	0.36
TiO_2	0.12
BaO	0.061
P_2O_5	0.037
SrO	0.032
MnO	0.029
ZrO_2	0.024
SO_3	0.021
Loss of ignition (LOI)	0.416

Efficiency of MAH Grafting

Samples in the form of films with thickness of about 200–300 μm were prepared by compression molding using a hot press at 150°C and pressure of 5 MPa. The films were vacuum dried at 75°C for 14 h to evaporate the unreacted MAH. FTIR spectrometer model Perkin Elmer System 2000 was used to record the FTIR spectra of the prepared films in the range of 500–4000 cm^{-1} and 0.4 cm^{-1} resolution.

Preparation of EPDM/MAH-*g*-EPDM/Bt Composites

Before the compounding, bentonite (Bt) was dried in oven at 80°C for 24 h to expel the moisture and MAH-*g*-EPDM was vacuum dried at 75°C for 4 h to evaporate the unreacted MAH. EPDM, MAH-*g*-EPDM and Bt were weighed based on the compounding formulation given in Table II along with a constant composition of zinc oxide (5 phr), stearic acid (1.5 phr), TMTD (1.5 phr), MBT (0.8 phr), and sulfur (1.5 phr) for all the compounds. The prepared compounding ingredients were mixed in laboratory scaled (160 × 320mm) two roll mill, model XK-160 according to American Standard of Testing Material (ASTM) designation D 3184-80. The curing behavior of composites was obtained using a Monsanto Moving Die Rheometer (MDR 2000) at 150°C. The curing time (t_{90}), scorch time (t_{S2}), maximum torque (M_H), and minimum torque (M_L) values were obtained from the rheograph. Based on the t_{90} values, the compounds are compression molded into sheets using hot press at the temperature of 150°C.

Measurement of Tensile Properties

Tensile tests were carried out on a dumb-bell shaped samples which was cut from compression molded sheets having a thickness of about 2 mm using a tensile specimen cutter after 24 h of storage upon hot press. The tensile strength, elongation at break (E_b), and tensile modulus at 100% ($M100$) elongation

Table II. Compounding Formulation of the EPDM/Bt Composites (phr)

	EPDM/Bt					EPDM/MAH-*g*-EPDM/Bt				
Composite	A1	A2	A3	A4	A5	B1	B2	B3	B4	B5
EPDM	100	100	100	100	100	90	90	90	90	90
MAH-*g*-EPDM	–	–	–	–	–	10	10	10	10	10
Bentonite	5	10	30	50	70	5	10	30	50	70

All composition in part per hundred rubber (phr).

were measured in accordance to ASTM D 412 using a Universal tensile testing machine Instron 3366 at room temperature (25 ± 2°C) at the crosshead speed of 500 mm/min.

Measurement of Solvent Resistance and Rubber-Filler Interaction

Samples with the dimensions of 30 × 5 × 2 mm were cut from the compression molded sheets and swelling tests were carried out using toluene as a solvent in accordance to ASTM D 471-79. The test pieces were weighed using an electronic balance and initial mass (M_i) of the specimens in gram were recorded. The test pieces were then immersed in toluene for 72 h and conditioned at 25°C, in dark place. After 72 h, the test pieces were weighed again and the mass of the specimens after immersion (M_s) in toluene were recorded. The test pieces are then dried in an oven at 70°C for 15 min and let cool at room temperature for another 15 min before the dry mass of the specimens (M_d) were weighed. Solvent resistance of composite was evaluated from the swelling percentage of composite in toluene. The lower swelling percentage indicates the higher solvent resistance of composite. Swelling percentage was calculated based on eq. (1).

$$\text{Swelling percentage} = \left[\frac{(M_s - Mi)}{M_i}\right] \times 100 \quad (1)$$

The rubber-filler interaction was obtained by applying Lorenz and Park equation and the swelling index was calculated based on eq. (2):

$$\frac{Q_f}{Q_g} = ae^{-z} + b \quad (2)$$

In this study, the weight of toluene uptake per gram of rubber hydrocarbon (Q) was determined according to eq. (3):

$$Q = \frac{[M_s - M_d]}{M_i \times 100/\text{Formula weight}} \quad (3)$$

where subscripts f and g in eq. (2) refers to the filled and gum vulcanizates, respectively; z is the ratio by weight of filler to rubber hydrocarbon in the vulcanizates; a and b are constants. The higher value of Q_f/Q_g indicates the lower extent of interaction between the filler and matrix.

Scanning Electron Microscopy Observation of the Tensile Fractured Surfaces

The morphologies of tensile fracture surface of EPDM/Bt composites with and without MAH-*g*-EPDM were observed under a ZEISS SUPRA™ 35VP Scanning electron microscope with GEMINI field emission column. The main purpose of this test is to observe the degree of dispersion of bentonite in the EPDM and to evaluate the interaction between bentonite and EPDM, with and without MAH-*g*-EPDM. Test specimens were placed in an aluminum mount with double sided sticky tape and coated with a thin layer of gold-palladium to eliminate electrostatic charging effects during the observation.

RESULT AND DISCUSSION

FTIR Analysis of MAH-*g*-EPDM

Figure 1 shows the FTIR spectra of pure EPDM and MAH-*g*-EPDM in the wavelength range of 4000–550 cm^{-1}. Vacuum drying of MAH-*g*-EPDM is required to eliminate the unreacted MAH which might give rise to the absorption bands in the same region as that of grafted anhydride does. The absence of absorption band at 700 cm^{-1} representing the C=C bonds of MAH confirms the complete reaction of MAH with EPDM or the elimination of unreacted MAH.[23,27] Comparing the FTIR spectra (a) pure EPDM and (b) MAH-*g*-EPDM, it is clearly seen that new absorption bands are formed upon the melt grafting of MAH onto EPDM rubber. As reported by Grigoryeva and Karger-Kocsis,[23] the absorption bands in the range of 1780–1792 cm^{-1} and 1850 cm^{-1} represents the symmetric and antisymmetric C=O stretching bonds, respectively. Meanwhile absorption band at 1713 cm^{-1} is attributed to the presence of dimeric carboxylic acid in MAH-*g*-EPDM.

Similar finding by Pasbakhsh et al.[27] reported that the absorption bands in the range of 1710–1719 cm^{-1} and 1770–1792 cm^{-1} represents the C=O symmetric stretching bonds in MAH-*g*-EPDM. Yaday[28] have reported that the absorption bands of O—H vibration of carboxylic acid dimers of MAH may also appear in the range on 2000–2700 cm^{-1}. Hence from Figure 1(a, b), the absorption peaks at 1845, 1774, and 1710 cm^{-1} gives a clear indication of the grafting of MAH onto EPDM chains. The absorption peak at 2670, 2310, and 2028 cm^{-1} represents the vibration of O—H bonds of the carboxylic acid dimers of the MAH. Besides that, other characteristic absorption bands for MAH also appear on the spectra at 1049 cm^{-1} (O=C—O—C=O vibrations in the cyclic anhydride), 1270 cm^{-1} (—C—O—C— stretching of ester bonds in MAH-*g*-EPDM) and 800–830 cm^{-1} (out-of-plane C—O bonding). The presence of OH group in MAH-*g*-EPDM is confirmed by the presence of absorption band in the range of 3600–3200, 1600, and 927 cm^{-1}.[27] According to Bussi and Simonazzi,[29] the absorption bands in the range of 760–680 cm^{-1} served as an internal standard which indicates the rocking-mode vibration of

Applied Polymer SCIENCE

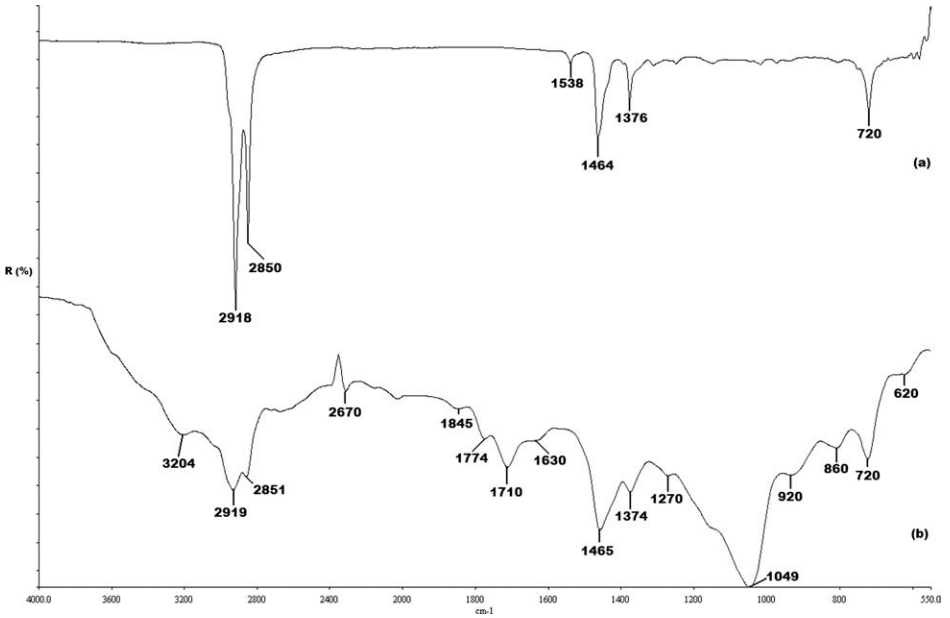

Figure 1. FTIR spectra of (a) pure EPDM and (b) MAH-*g*-EPDM.

longer methylene sequences [—$(CH_2)_n$—. with $n \geq 5$ and this absorption bands appears in both pure EPDM and MAH-*g*-EPDM at 720 cm^{-1}.

CURING BEHAVIOR

Table III shows the curing characteristics of compatibilized (EPDM/MAH-*g*-EPDM/Bt) and uncompatibilized (EPDM/Bt) composites. From the results obtained, it can be concluded that addition of 10 phr of MAH-*g*-EPDM have increased the curing time (t_{90}), scorch time (t_{S2}), maximum torque (M_H), and minimum torque (M_L) of EPDM/Bt composites. At similar Bt loading, the t_{90} and t_{S2} of compatibilized EPDM/Bt composites are higher than that of uncompatibilized composites. It was reported earlier by Pasbakhsh et al.[27] that MAH is capable of retarding the curing process by reacting with accelerator species causing in prolonged optimum cure time and scorch time. On the other hand, report by Manjhi and Sarkhel[1] stated that MAH-*g*-EPDM introduces acidic carbonyl groups which may react and decompose sulfur into ions instead of radicals and this inhibits the curing process and increases the optimum cure time. Therefore, it can be said that the increase of t_{90} and t_{S2} of compatibilized EPDM/Bt composites were caused by the cure retardancy effect of MAH.

Incorporations of MAH-*g*-EPDM increase the interfacial interaction between EPDM and Bt and this can be seen from the increasing M_H and M_L values. Both torque values of compatibilized EPDM/Bt composites were higher than that of uncompatibilized EPDM/Bt composites at similar Bt loadings. The improvement of interfacial interaction between EPDM and Bt in the presence of MAH-*g*-EPDM reduce the mobility of Bt particles and increases the stiffness of compound resulting in higher shearing effect corresponding to increases torque. Increase in M_L value indicates the lower processability of compatibilized EPDM/Bt composites compared with uncompatibilized EPDM/Bt composites due to increase in the shearing effect which complicates the compounding process.

Table III also shows the effect of Bt loading on the curing characteristics of EPDM/Bt composites which was discussed in our previous study.[22] The curing time is decreased from 5 to 30 phr of Bt loading which increased again at 50 and 70 phr. The absorption of zinc oxide and accelerator on the surface of Bt and entrapment of EPDM in between Bt aggregates affects the curing process. Below 30 phr of Bt loading, the absorption of zinc oxide and accelerator are not significant, accelerating the curing process. However at higher Bt loading, more accelerators would be absorbed, reducing the amount of sulfurating agent, which prolongs the vulcanization process.

Tensile Properties

Figure 2 shows the comparison between tensile strength of MAH-*g*-EPDM compatibilized and uncompatibilized EPDM/Bt

Table III. Curing Characteristics of EPDM/Bt Composites

Sample coding	t_{90} (min)	t_{S2} (min)	M_H (dN m)	M_L (dN m)
Unfilled EPDM	21.32	6.52	16.57	1.33
EPDM/5Bt	18.32	2.48	16.74	1.58
EPDM/5Bt/MAH-*g*-EPDM	19.42	3.44	16.94	1.60
EPDM/10Bt	17.88	1.68	17.19	1.85
EPDM/10Bt/MAH-*g*-EPDM	18.51	2.21	18.24	2.03
EPDM/30Bt	16.58	1.11	18.37	2.20
EPDM/30Bt/MAH-*g*-EPDM	17.39	1.45	19.14	2.52
EPDM/50Bt	24.12	2.04	19.24	3.01
EPDM/50Bt/MAH-*g*-EPDM	24.81	2.52	20.06	3.41
EPDM/70Bt	24.96	3.17	16.43	3.11
EPDM/70Bt/MAH-*g*-EPDM	25.90	3.89	21.05	3.64

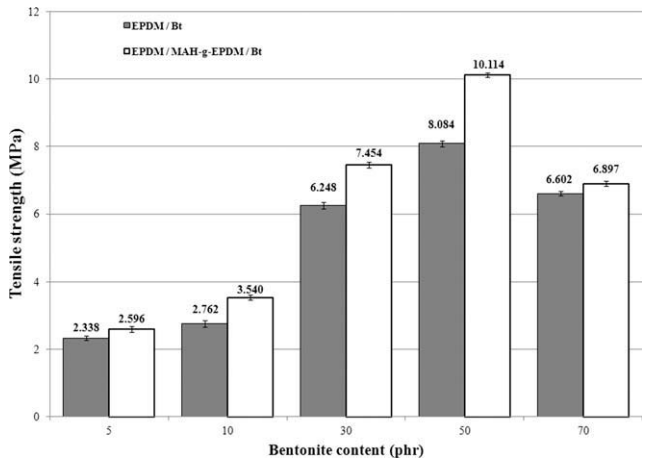

Figure 2. Tensile strength of EPDM/Bt and EPDM/MAH-*g*-EPDM/Bt composites.

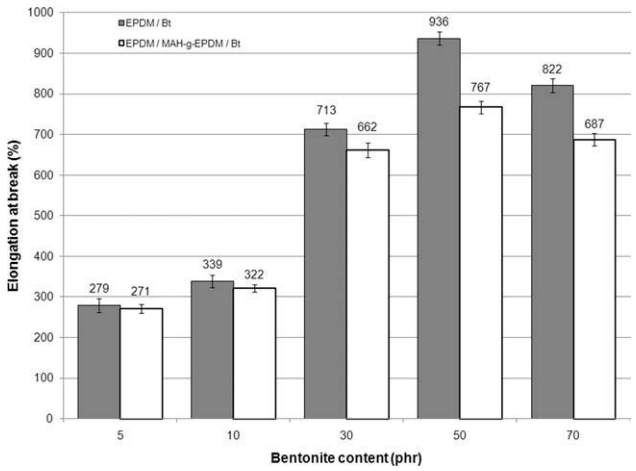

Figure 4. Elongation at break of EPDM/Bt and EPDM/MAH-*g*-EPDM/Bt composites.

composites with increasing Bt loading from 5 to 70 phr. Tensile strength of the compatibilized EPDM/Bt composites are higher compared with uncompatibilized EPDM/Bt composites at all the Bt loadings. The increment of tensile strength in the presence of MAH-*g*-EPDM is due to the formations of hydrogen bonds between EPDM and Bt particles at the interfacial. Figure 3 shows the possible reinforcement mechanism of EPDM by Bt due to MAH-*g*-EPDM compatibilization. MAH reacts with EPDM in the presence of DCP to form an intermediate molecule which forms hydrogen bonding to the hydroxyl (—OH) groups at the surface of Bt.

According to Manjhi and Sarkhel,[1] Van Der Waals type of bonding is formed between the MAH-*g*-EPDM and clay due to the delocalized free electrons on the vicinity of filler. The anhydride groups on the maleated rubber will interact with the oxygen atom on the surface of clay and forms bridge bonding via free radical mechanism. Besides that, the dispersion of Bt particles in EPDM matrix also influence the tensile strength of EPDM/Bt composites which was increased in the presence of MAH-*g*-EPDM which further increases the interfacial interaction between EPDM and Bt particles to give a higher tensile strength.

Purnima et al.[30] stated that tensile strength and modulus increased with greater interfacial adhesion between the components of a blend. The tensile strength of both compatibilized and uncompatibilized EPDM/Bt composites were decreased with addition of 70 phr Bt loading compared with 50 phr Bt

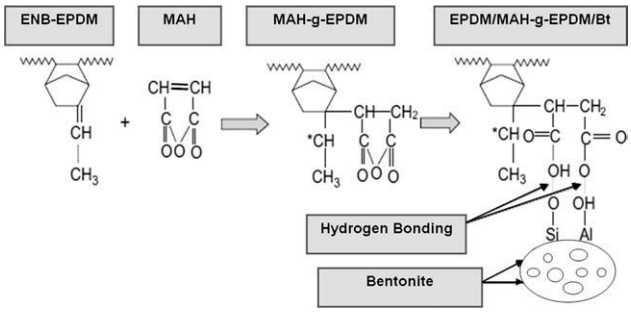

Figure 3. Possible reinforcement mechanism of EPDM/Bt by MAH-*g*-EPDM.

loading. As discussed in our previous study,[22] agglomerations of Bt particle were observed at higher Bt loading which responsible for the decreased in tensile strength. However, incorporation of MAH-*g*-EPDM has improved the dispersion of Bt particles at 70 phr Bt loading and higher tensile strength of compatibilized EPDM/Bt composite was obtained in comparison with uncompatibilized EPDM/Bt composite, which will be further discussed in the SEM morphological observations.

Figure 4 illustrates the elongation at break (E_b) of EPDM/Bt and EPDM/MAH-*g*-EPDM/Bt composites at Bt loading of 5–70 phr. As shown at Figure 4, the E_b of compatibilized EPDM/Bt composite is lower than that of uncompatibilized EPDM/Bt composites at all the Bt loadings. As discussed earlier, addition of MAH-*g*-EPDM enhances the dispersion of Bt dispersion in EPDM matrix and interfacial interaction between EPDM and Bt. Enhancement of Bt particles and interfacial interaction increases the composite stiffness and in return decreases the E_b of compatibilized EPDM/Bt composites compared with uncompatibilized EPDM/Bt composites.

Tensile modulus at 100% elongation ($M100$) of the EPDM/Bt and EPDM/MAH-*g*-EPDM/Bt composites at Bt loading of 5–70 phr is demonstrated in Figure 5. As can be seen, $M100$ of EPDM/Bt composite is increased in the presence of MAH-*g*-EPDM compared with uncompatibilized EPDM/Bt composites. The presence of MAH groups in MAH-*g*-EPDM forms stronger bonding to Bt surface and this enhances the interfacial interaction between EPDM and Bt. As discussed before, the enhancement of interfacial interaction between EPDM and Bt increases the stiffness of compatibilized EPDM/Bt composite compared with uncompatibilized EPDM/Bt composites. This result is in line with the increasing torque value of EPDM/MAH-*g*-EPDM/Bt composites indicating the increase in shearing effect due to stiffening of EPDM/Bt composites in the presence of MAH-*g*-EPDM. Similar finding was reported by Mohammadpour and Katbab,[21] at which the degree of reinforcement was very significant with the incorporation of MAH-*g*-EPDM as compatibilizer in organomodified montmorillonite (OMMT) filled EPDM nanocomposites.

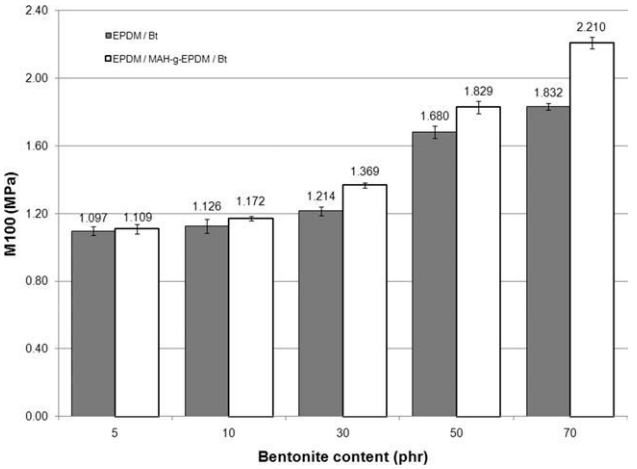

Figure 5. *M*100 of EPDM/Bt and EPDM/MAH-*g*-EPDM/Bt composites.

Scanning Electron Microscopy

Figure 6(a–d)represents the tensile fractured surfaces of EPDM/Bt and EPDM/MAH-*g*-EPDM/Bt composites. Figure 6(a, c) is the SEM micrographs of tensile fractured surface of EPDM/30Bt and EPDM/MAH-*g*-EPDM/30Bt composite, it can be clearly seen that Bt particles are well dispersed in the presence of MAH-*g*-EPDM compared with that of the uncompatibilized EPDM/Bt composite. It is also observed that the matrix tearing and surface roughness increased in the presence of MAH-*g*-EPDM compared with the uncompatibilized EPDM/Bt composite. The increased surface roughness and matrix tearing of the fractured surface proves the enhancement of the interfacial interaction between Bt and EPDM in the presence of MAH-*g*-EPDM. This observation is in good agreement with the higher tensile properties of compatibilized EPDM/Bt composites. The presence of MAH in EPDM/MAH-*g*-EPDM/Bt composites enhances the dispersion of Bt particles with increasing Bt loading as shown by Figure 6(c, d).

Agglomeration of Bt particles were observed at higher Bt loading of EPDM/70Bt composite as shown in Figure 6(b). At higher Bt loading, the space between particles were minimized which increases the interaction in between Bt particles. Without MAH-*g*-EPDM, Bt particles were not well dispersed and this results in low tensile properties of the uncompatibilized EPDM/Bt composites at all Bt loadings. However, incorporation of MAH-*g*-EPDM enhances the dispersion of Bt particles in

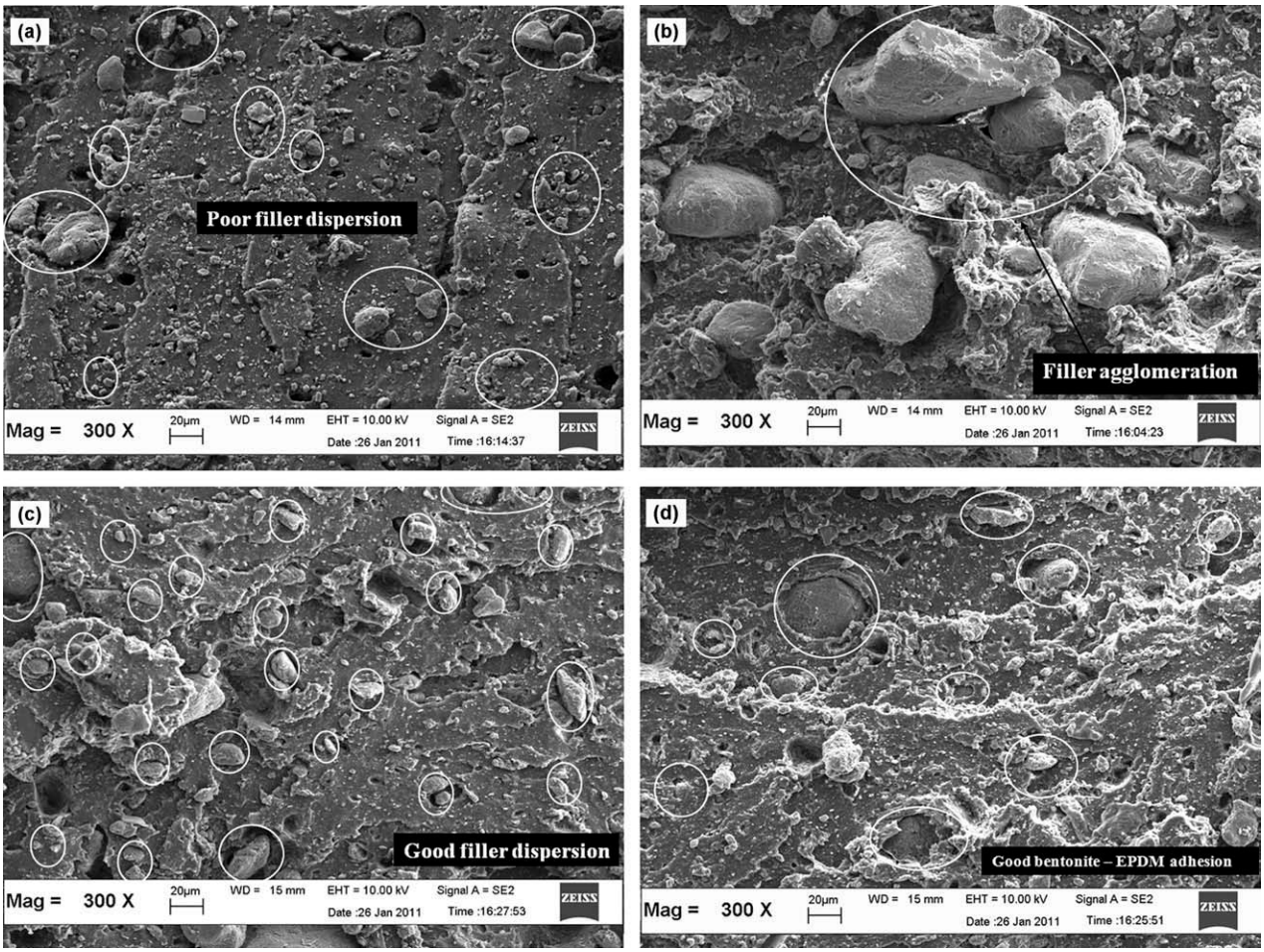

Figure 6. SEM micrographs of tensile fractured surface of EPDM/Bt composites: (a) EPDM/30Bt, (b) EPDM/70Bt; and EPDM/MAH-*g*-EPDM/Bt composites: (c) EPDM/MAH-*g*-EPDM/30Bt, (d) EPDM/MAH-*g*-EPDM/70Bt.

EPDM/MAH-*g*-EPDM/70Bt composite as shown in Figure 6(d). Good adhesion between Bt and EPDM can be observed in the presence of MAH-*g*-EPDM indicating the enhanced interfacial interaction between Bt and EPDM matrix at higher Bt loading.

Solvent Resistance of EPDM/Bt Composites in Toluene

The effect of compatibilization of EPDM/Bt composites by MAH-*g*-EPDM on the swelling percentage is shown in Figure 7. Swelling percentage based on toluene uptake is a measure of the solvent resistance and degree of crosslinking. The reduction in swelling percentage indicates a greater solvent resistance and increasing crosslink density of the composite material. As can be seen from Figure 7, the comparison between the swelling percentages of compatibilized and uncompatibilized EPDM/Bt composites indicates the better chemical stability of compatibilized EPDM/Bt composites at all the Bt loadings. Improvement in solvent resistance of compatibilized EPDM/Bt composites in the presence of MAH-*g*-EPDM proves the better interfacial interaction between EPDM and Bt particles. Swelling percentage of both the composites is decreased with the increasing Bt loading up to 50 phr Bt loading and slightly increased at higher Bt loading of 70 phr.

This result is in good agreement with the tensile properties obtained at which increasing tensile properties up to 50 phr Bt loading were obtained for both the composites due to well dispersion of Bt and good interfacial interaction between EPDM and Bt. EPDM might form a protective layer at the interface of Bt and prevents the diffusion of toluene into Bt. However, agglomeration and high interaction in between Bt particles increased the swelling percentage at 70 phr Bt loading for uncompatibilized EPDM/Bt composite and slightly better swelling resistance were observed in the presence of MAH-*g*-EPDM at similar Bt loading for compatibilized EPDM/Bt composite. Besides that, it is believed that the presence of hydrogen bonds between Bt and EPDM via MAH groups increases the ability of EPDM to extend upon the toluene diffusion. Sombatsompop[31] and Valadares et al.[32] have reported that increasing interaction between rubber and montmorillonite will result in increasing crosslink sites of the composite and subsequently reduce the solvent uptake which increases the solvent resistance of the composite.

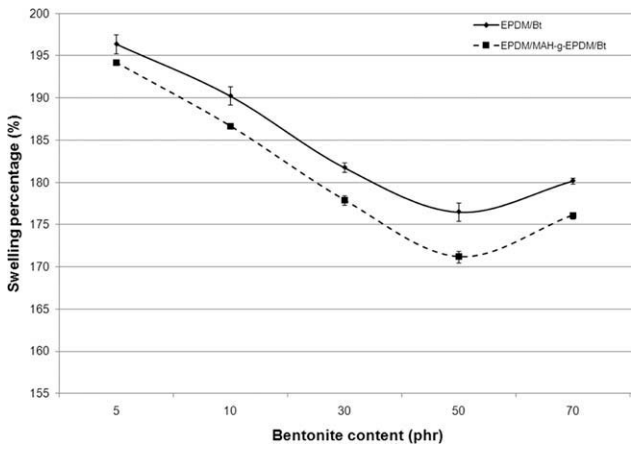

Figure 7. Swelling percentage of EPDM/Bt and EPDM/MAH-*g*-EPDM/Bt composites.

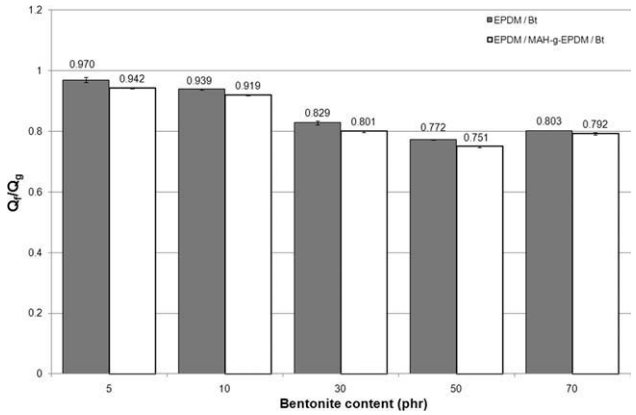

Figure 8. Q_f/Q_g values of the EPDM/Bt and EPDM/MAH-*g*-EPDM/Bt composites.

Rubber–Filler Interaction

The effect of MAH-*g*-EPDM compatibilization on the rubber–filler interaction (Q_f/Q_g) of EPDM/Bt composites at Bt loading of 5–70 phr is shown in Figure 8. It can be seen that Q_f/Q_g of the compatibilized EPDM/Bt composites is higher than that of uncompatibilized EPDM/Bt composites at all the Bt loadings examined. Enhancement of Bt dispersion and interfacial interaction between EPDM and Bt in the presence of MAH-*g*-EPDM results in improved rubber–filler interaction. The Q_f/Q_g of both composites are decreased with the increasing Bt loading up to 50 phr and increased slightly at 70 phr Bt loading. This indicates that incorporation of MAH-*g*-EPDM has increased the interaction between EPDM and Bt and the decrease in the toluene uptake is also a sign of improvement in rubber–filler interaction. According to Ismail and Shaari,[33] the enhancement of interaction between EPDM and filler would increase the possibility of forming more crosslink density per unit rubber chain. Hence, increase in crosslink density will decrease the toluene up take which attribute to the higher rubber–filler interaction. Besides that, as discussed earlier, the presence of MAH group in EPDM/MAH-*g*-EPDM/Bt composites, introduces hydrogen bonding with the oxygen atoms at Bt surface and this further improves the interaction between EPDM and Bt.

CONCLUSIONS

MAH-*g*-EPDM has been successfully prepared through melt blending of EPDM, MAH and DCP and the presence of anhydride groups in EPDM was proved by FTIR analysis. Compatibilization of EPDM/Bt composites with MAH-*g*-EPDM has increased the cure time, scorch time, maximum torque, and minimum torque of the EPDM/MAH-*g*-EPDM/Bt composites at all Bt loading. Tensile strength and modulus at 100% elongation ($M100$) of compatibilized composites are increased, whereas the elongation at break is decreased compared with uncompatibilized EPDM/Bt composites. Decreased swelling percentage and increasing rubber–filler interactions indicates the enhancements of interfacial interaction of EPDM and Bt and better adhesion of Bt to EPDM matrix in the presence of

MAH-*g*-EPDM compatibilizer. SEM study shows the evidence in increasing interfacial interaction between EPDM and BT via increasing roughness and matrix tearing, and well dispersion of Bt particle in EPDM matrix of compatibilized EPDM/Bt composites.

ACKNOWLEDGMENTS

The author would like to thank Universiti Sains Malaysia for the financial support under USM fellowship scheme for his MSc study.

REFERENCES

1. Manjhi, S.; Sarkhel, G. J. *Appl. Polym. Sci.* **2011,** *119*, 2268.
2. Qingjun, D.; Guohui, W.; Baolei, L.; Wei, Z.; Baixing, H.; Jian, S. *Polym. Compos.* **2005,** *26*, 587.
3. Ismail, H.; Pasbakhsh, P.; Ahmad Fauzi, M. N.; Abu Bakar, A. *Polym. Test.* **2008,** *27*, 841.
4. Hoffman, W. Rubber Technology Handbook; Oxford University Press: New York, **1989.**
5. Ciesielski, A. An Introduction to Rubber Technology; Rapra Technology Ltd: Southampton, **1999.**
6. Lee, C. H.; Kim, S. W. J. *Appl. Polym. Sci.* **2000,** *78*, 2540.
7. Hamza, S. S. *Polym. Test.* **1998,** *17*, 131.
8. Zheng, H.; Zhang, Y.; Peng, Z.; Zhang, Y. *Polym. Test.* **2004,** *23*, 217.
9. Harper, C. A.; Petrie, E. M. Plastics Materials and Processes: A Concise Encyclopedia; John Wiley & Sons Inc: New Jersey, **2003.**
10. Arroyo, M.; Lopez-Manchado, M. A.; Herrero, B. *Polymer* **2003,** *44*, 2447.
11. Poh, B. T.; Ismail, H.; Tan, K. S. *Polym. Test.* **2002,** *21*, 801.
12. Ismail, H.; Chia, H. H. *Polym. Test.* **1998,** *17*, 199.
13. Ismail, H.; Ramli, R. J. *Reinforc. Plast. Compos.* **2008,** *27*, 1909.
14. Lu, Y. L.; Li, Z.; Yu, Z. Z.; Tian, M.; Zhang, L. Q.; Mai, Y. W. *Compos. Sci. Technol.* **2007,** *67*, 2903.
15. Waddell, W. H.; Evans, L. R. *Rubber Chem. Technol.* **1996,** *69*, 377.
16. Theng, B.K. G. *Clay Clay Miner.* **1970,** *18*, 357.
17. Usuki, A.; Tukigase, A.; Kato, M. *Polymer* **2002,** *43*, 2185.
18. Vu, Y. T.; Mark, J. E.; Pham, L. H.; Engelhardt, M. J. *Appl. Polym. Sci.* **2001,** *82*, 1391.
19. Kresge, E. N.; Lohse, D. J. US Pat. 5,576,372, **1996.**
20. Chang, Y. W.; Yang, Y.; Ryu, S.; Nah, C. *Polym. Int.* **2002,** *51*, 319.
21. Mohammadpour, Y.; Katbab, A. A. *J. Appl. Polym. Sci.* **2007,** *106*, 4209.
22. Ismail, H.; Mathialagan, M. *Polym.-Plast. Technol. Eng.* **2011,** *50*, 1421.
23. Grigoryeva, O.; Karger-Kocsis, J. *Eur. Polym. J.* **2000,** *36*, 1419.
24. Hu, G.; Wang, B.; Zhou, X. *Mater. Lett.* **2004,** *58*, 3457.
25. Chakrit, S.; Sauvarop, L.; Jarunee, T. J. *Appl. Polym. Sci.* **2003,** *89*, 1156.
26. Deanin, R. D.; Mathur, S. ANYEC Conf. Proc. **2003,** *2*, 2714.
27. Pasbakhsh, P.; Ismail, H.; Ahmad Fauzi, M. N.; Abu Bakar, A. *Polym. Test.* **2009,** *28*, 548.
28. Yaday, L.D. S. Organic Spectroscopy; Kluwer Academic Publisher: New Delhi, **2005.**
29. Bussi, G.; Simonazzi, T. J. *Polym. Sci. Part C* **1964,** *7*, 203.
30. Purnima, D.; Maiti, S. N.; Gupta, A. K. *J. Appl. Polym. Sci.* **2006,** *102*, 5528.
31. Sombatsompop, N. *Polym.-Plast. Technol. Eng.* **1998,** *37*, 19.
32. Valadares, L. F.; Leite, C. A. P.; Galembeck, F. *Polymer* **2006,** *47*, 672.
33. Ismail, H.; Shaari S. M. *Polym. Test.* **2010,** *29*, 872.